

Synthesis, Characterization, and Biological Activity of New 4'-Functionalized Bis-Terpyridine Ruthenium(II) Complexes: Anti-Inflammatory Activity Advances

Mohamed M. Elnagar,^{*[a, b]} Khaled S. Abou-El-Sherbini,^[b] Safia Samir,^[c] Walid Sharmoukh,^[b] Mohamed S. Abdel-Aziz,^[d] and Yasser M. Shaker^{*[e]}

Ruthenium complexes incorporating 2,2':6',2''-terpyridine ligands have emerged as promising candidates due to their versatile biological activities including DNA-binding, anti-inflammatory, antimicrobial, and anticancer properties. In this study, three new 4'-functionalized bis(terpyridine) Ru(II) complexes were synthesized. These complexes feature one ligand as 4-(2,2':6',2''-terpyridine-4'-yl) benzoic acid and the second ligand as either 4'-(2-thienyl)-2,2':6',2''-terpyridine, 4'-(3,4-dimethoxyphenyl)-2,2':6',2''-terpyridine, or 4'-(4-dimethylaminophenyl)-2,2':6',2''-terpyridine. Besides the chemical characterization by ¹H and ¹³C NMR, mass spectrometry, and absorption and emission spectroscopy, the complexes were tested for their biological activity as anti-inflammatory, anticancer, and anti-

microbial agents. Moreover, the toxicity of the Ru(II) complexes was assessed and benchmarked against diclofenac potassium and ibuprofen using a haemolysis assay. Biological evaluations demonstrate that these ruthenium complexes exhibit promising therapeutic potential with reduced haemolytic activity compared to standard drugs. They demonstrate substantial anti-inflammatory effects through inhibition of albumin denaturation along with moderate cytotoxicity against cancer cell lines and broad-spectrum antimicrobial activity. These findings highlight the multifaceted biomedical applications of 4'-functionalized bis(terpyridine) Ru(II) complexes, suggesting their potential for further development as effective and safe therapeutic agents.

Introduction

The design and synthesis of new metal-organic coordination compounds as metallotherapeutic drugs have garnered significant interest due to their multiple therapeutic functionalities, which are often not achievable with traditional organic molecules.^[1,2] Polypyridyl ruthenium complexes, in particular, are pivotal in therapeutic developments due to their unique

characteristics, such as rapid ligand exchange, different oxidation states, and ruthenium's capability to imitate iron in binding to specific biological targets. Consequently, this class of metal complexes exhibits high biological activity, including DNA binding, anti-inflammatory, antimicrobial, and anticancer properties.^[3–8] In particular, 2,2':6',2''-terpyridines (terpy or tpy) (Figure 1A) as N-heterocycles are of great significance because of their exceptional ability to form stable complexes. The presence of three connected pyridine units, which contain three tertiary ring nitrogen donor atoms, grants these ligands a high chelating ability.^[9] The core pyridine ring stabilizes the planar structure through intramolecular hydrogen bonds (CH...N) involving core and peripheral pyridine rings, as shown in structure B (Figure 1B).^[10] These nitrogen donor atoms form M–N_{pyridine} bonds in transition metal complexes, where the σ -donor/ π -acceptor nature of these bonds provides high stability via $d\pi$ – $p\pi^*$ back bonding.^[11] Moreover, 2,2':6',2''-terpyridine ligands form octahedral geometric structures upon coordination with metal centers using the $\langle tpy-M^{II}-tpy \rangle$ connection, leading to M^{II}-bis-terpyridine complexes. This family of rigid, well-defined complexes is typically synthesized through two consecutive steps. The incorporation of two tpy units to the metal ion center results in fascinating photophysical characteristics and enhances the therapeutic activity of these complexes.^[12,13]

Currently, many available non-steroidal anti-inflammatory drugs (NSAIDs) demonstrate high therapeutic efficacy by selectively inhibiting COX-2 (coxibs) without affecting COX-1 enzymatic activity.^[14–16] However, despite their selective inhibition, potential cardiovascular side effects have brought these

[a] M. M. Elnagar
Institute of Electrochemistry, Ulm University, Albert-Einstein-Allee 47, 89081 Ulm, Germany
E-mail: mohamed.elnagar@uni-ulm.de

[b] M. M. Elnagar, K. S. Abou-El-Sherbini, W. Sharmoukh
Department of Inorganic Chemistry, National Research Centre, 33 El Bohouth St. (former Tahrir St.), 12622 Dokki, Giza, Egypt

[c] S. Samir
Department of Biochemistry and Molecular Biology, Theodor Bilharz Research Institute, P.O. Box 30, Giza, Egypt

[d] M. S. Abdel-Aziz
Department of Microbial Chemistry, National Research Centre, 33 El Bohouth St. (former Tahrir St.), 12622 Dokki, Giza, Egypt

[e] Y. M. Shaker
Division of Pharmaceutical and Drug Industries, Department of the Chemistry of Natural and Microbial Products, National Research Centre, El Bohouth Street, Dokki, Cairo 12622, Egypt
E-mail: yabdelrahman11@yahoo.com

Supporting information for this article is available on the WWW under <https://doi.org/10.1002/cmdc.202400680>

© 2024 The Authors. ChemMedChem published by Wiley-VCH GmbH. This is an open access article under the terms of the Creative Commons Attribution License, which permits use, distribution and reproduction in any medium, provided the original work is properly cited.

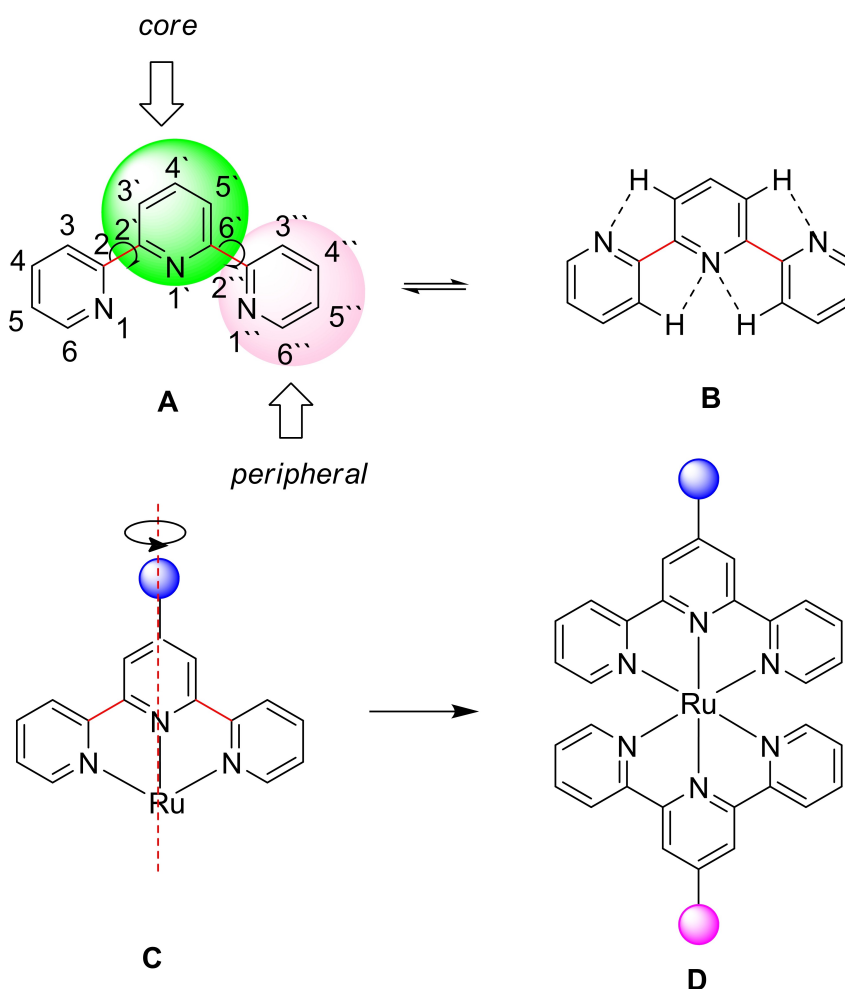


Figure 1. 2,2':6',2''-Terpyridines (tpty) (A); stabilization of the planar structure of tpty by the core pyridine ring through intramolecular hydrogen bonds (B); the stability and symmetry of the synthesized Ru(II) complex (C); and the designed structure of bis(terpyridine) Ru(II) complexes with different functionalization at the 4'-position (D).

drugs under scrutiny.^[17,18] Additionally, inflammation can promote bacterial growth due to fluid accumulation in injured areas, necessitating the simultaneous prescription of separate anti-inflammatory and antimicrobial drugs, complicating NSAID therapy.^[19] Chronic inflammation also predisposes individuals to cancer development and tumor progression, and treatment resistance is particularly facilitated by chronic inflammation.^[20,21] Furthermore, inflammation is a key feature of COVID-19.^[22] Given these challenges, designing new, more potent, and safer compounds with combined anti-inflammatory, antimicrobial, and anticancer effects is of paramount importance. Ruthenium complexes have established themselves as active metallochemotherapeutic agents, not only as derivatives of NSAIDs but also in exhibiting antimicrobial activity against drug-resistant pathogens.^[3,23,24]

The development and antibacterial activity of 2,2':6',2''-terpyridine and bis(terpyridine) metal complexes [metal = ruthenium (II) and rhodium (III)] have been achieved, with some complexes showing superior activity compared to commercially available antibiotics such as kanamycin and streptomycin (Figure 1C).^[25] Functionalization of bis-terpyridine at the 4'-position

enables the design of systems with donor and acceptor groups in opposite directions (Figure 1D). Most NSAIDs contain carboxylic groups as hydrophilic elements and aromatic rings as lipophilic groups, creating an amphiphilic structure. This amphiphilic nature is crucial for the synergistic effect on cellular uptake and phototoxicity, and for the permeation through bacterial cell walls.^[26]

In light of these aspects, and continuing our previous work on synthesizing 2,2':6',2''-terpyridine Ru(II) complexes as anti-inflammatory agents,^[27] this study aims to synthesize new 4'-functionalized bis(terpyridine) Ru(II) complexes with improved biological activity. In this regard, new heteroleptic Ru(II)-complexes have been successfully synthesized in two steps, featuring one ligand as 4-(2,2':6',2''-terpyridine-4'-yl) benzoic acid, and the second ligand as either 4'-(2-thienyl)-2,2':6',2''-terpyridine, 4'-(3,4-dimethoxyphenyl)-2,2':6',2''-terpyridine, or 4'-(4-dimethylaminophenyl)-2,2':6',2''-terpyridine. The anti-inflammatory, cytotoxic, and antimicrobial activities of these synthesized Ru(II) complexes were systematically evaluated, revealing how variations in the 4'-substituents of the terpyridine motif affect their biological activity. Notably, these complexes

demonstrate a wide range of robust biological activities. Furthermore, they have low haemolytic potential, effectively inhibit heat-induced albumin denaturation to reduce inflammation, selectively target cancer cells, and possess broad-spectrum antimicrobial properties. More importantly, the Ru(II) complex featuring a 3,4-dimethoxyphenyl group on the terpyridine stands out as the most promising, exhibiting the highest anti-inflammatory activity and remarkable antimicrobial effectiveness against various pathogens.

Experimental Section

Chemicals and Solvents

All chemicals including 2-acetylpyridine (Sigma-Aldrich, $\geq 99\%$), thiophene-2-carbaldehyde (Sigma-Aldrich, 98%), 3,4-dimethoxybenzaldehyde (Alfa-Aesar, 99%), 4-(dimethylamino)benzaldehyde (Sigma-Aldrich, 98%) or 4-methylbenzaldehyde (Across, 97%), ruthenium(III) chloride hydrate (Sigma-Aldrich, $\geq 99.9\%$), ammonium hexafluorophosphate (NH_4PF_6) (Thermo Scientific Chemicals, 99.5%) were utilized as received. All solvents were of HPLC grade and used directly without further purification.

Characterization

^1H NMR and ^{13}C NMR spectra were obtained using Bruker 500 MHz instruments using the residual signals for CDCl_3 at 7.26 and 77.0 ppm and for $\text{DMSO}-d_6$ at 2.50 and 39.4 ppm as internal references for ^1H and ^{13}C , respectively. High-resolution mass spectrometry (HRMS) was conducted on an asolariX (Bruker Daltonik) with a 7.0 T superconducting magnet and interfaced to an Apollo II Dual ESI/MALDI source. UV-vis spectra were captured with a PerkinElmer Lambda 750 UV-vis spectrophotometer, while emission spectra were measured using a FP-6500 spectrofluorometer (Jasco, Japan).

Synthesis

Synthesis of the Ligands

The ligands 4'-(*p*-tolyl)-2,2':6',2''-terpyridine, 4'-(4-dimethylaminophenyl)-2,2':6',2''-terpyridine, 4'-(2-thienyl)-2,2':6',2''-terpyridine, and 4'-(3,4-dimethoxyphenyl)-2,2':6',2''-terpyridine were synthesized following established literature methods.^[28,29] Detailed synthesis procedures are demonstrated in the supporting information. ^1H NMR and ^{13}C NMR spectra of the ligands are displayed in Figure S1.

Synthesis of the Ru(II) Complexes

The Ru(tpy)Cl₃ complexes were synthesized as following; terpyridine ligand (4'-(4-dimethylaminophenyl)-2,2':6',2''-terpyridine, 4'-(2-thienyl)-2,2':6',2''-terpyridine, or 4'-(3,4-dimethoxyphenyl)-2,2':6',2''-terpyridine) was reacted with $\text{RuCl}_3 \cdot 3\text{H}_2\text{O}$ in dry methanol for 6 h. After the reaction, the methanol was removed by evaporation under reduced pressure. The product was then filtered with cold methanol, and the resulting solid was dried. This solid was subsequently reacted with the ligand 4'-([2,2':6',2''-terpyridine]-4'-yl)benzoic acid in 10 ml of DMF for 6 h. The product was precipitated by adding the reduced volume of the DMF reaction mixture to an excess of saturated aqueous NH_4PF_6 solution. The

resulting solid was filtered, washed with distilled water and diethyl ether, and dried under vacuum. The yields of (4'-([2,2':6',2''-terpyridine]-4'-yl)benzoic acid) Ru(II)di(hexafluoro- λ^6 -phosphane), (4'-(3,4-dimethoxyphenyl)-2,2':6',2''-terpyridine) (4'-([2,2':6',2''-terpyridine]-4'-yl)benzoic acid) Ru(II)di(hexafluoro- λ^6 -phosphane), and (4'-([2,2':6',2''-terpyridine]-4'-yl)-N,N-dimethylaniline) (4'-([2,2':6',2''-terpyridine]-4'-yl)benzoic acid) Ru(II)di(hexafluoro- λ^6 -phosphane) are 62%, 65%, and 70%, respectively. The NMR spectra of the Ru(II) complexes are displayed in Figure S2, and the mass spectra are demonstrated in Figure S3.

(4'-(Thiophen-2-yl)-2,2':6',2''-terpyridine) (4'-([2,2':6',2''-terpyridin]-4'-yl)benzoic acid) Ru(II) di(hexafluoro- λ^6 -phosphane)

^1H NMR (400 MHz, DMSO) δ 9.52 (s, 2H, C_{3-H}), 9.34 (s, 2H, C_{5-H}), 9.14 (dd, $J=21.7$, 8.1 Hz, 4H, C_{4-H}, C_{4'-H}), 8.44 (dd, $J=18.8$, 5.4 Hz, 4H, C_{5-H}, C_{5'-H}), 8.20 (d, $J=7.9$ Hz, 4H, C_{6-H}, C_{6'-H}), 8.07 (t, $J=7.8$ Hz, 4H, C_{3-H}, C_{3'-H}), 8.03 (d, $J=5.1$ Hz, 2H, Ar-H), 7.64 – 7.53 (m, 2H, thiophene-H), 7.53 – 7.42 (m, 2H, Ar-H), 7.29 (s, 1H, thiophene-H) ppm.

^{13}C NMR (100 MHz, DMSO) δ 168.10, 158.54, 158.28, 155.55, 155.49, 152.71, 147.36, 141.39, 140.48, 138.52, 130.74, 130.39, 129.73, 129.24, 128.30, 128.17, 127.28, 125.38, 121.58, 119.89 ppm.

MS (MALDI) m/z calcd for $[\text{C}_{41}\text{H}_{28}\text{F}_{12}\text{N}_6\text{O}_2\text{P}_2\text{RuS}]$ (M)⁺: 1060.0322, found 1060.2122.

(4'-([2,2':6',2''-Terpyridin]-4'-yl)-N,N-dimethylaniline) (4'-([2,2':6',2''-terpyridin]-4'-yl)benzoic acid) Ru(II) di(hexafluoro- λ^6 -phosphane)

^1H NMR (400 MHz, DMSO) δ 9.44 (s, 2H, C_{3-H}), 9.30 (s, 2H, C_{5-H}), 9.04 (dd, $J=15.2$, 8.10 Hz, 4H, C_{4-H}, C_{4'-H}), 8.40 (d, $J=8.20$ Hz, 4H, C_{5-H}, C_{5'-H}), 8.29 (d, $J=8.8$ Hz, 4H, C_{6-H}, C_{6'-H}), 8.17 (d, $J=8.0$ Hz, 4H, C_{3-H}, C_{3'-H}), 7.98 (d, $J=5.1$ Hz, 2H, Ar-H), 7.47 (m, 2H, Ar-H), 7.30–7.10 (m, 2H, Ar-H), 6.93 (d, $J=8.9$ Hz, 2H, Ar-H), 3.05 (s, 6H, N(CH₃)₂) ppm.

^{13}C NMR (101 MHz, DMSO) δ 167.88, 162.79, 158.75, 158.56, 155.82, 155.03, 152.70, 152.19, 147.97, 138.42, 130.50, 129.08, 128.27, 128.01, 127.77, 125.30, 122.74, 121.67, 119.57, 112.59, 36.25, 31.24 ppm.

MS (MALDI) m/z calcd for $[\text{C}_{45}\text{H}_{35}\text{F}_{12}\text{N}_7\text{O}_2\text{P}_2\text{Ru}]$ (M)⁺: 1097.1179, found 808.1645 $[\text{M} + 1 - 2\text{PF}_6^-]$. PF_6^- units can be lost upon MALDI which is accompanied by electron capture and lower the mass by (145 for each PF_6 unit).

(4'-(3,4-Dimethoxyphenyl)-2,2':6',2''-terpyridine) (4'-([2,2':6',2''-terpyridin]-4'-yl)benzoic acid) Ru(II) di(hexafluoro- λ^6 -phosphane)

^1H NMR (400 MHz, DMSO) δ 9.53 (s, 2H, C_{3-H}), 9.41 (s, 2H, C_{5-H}), 9.16 (d, $J=14.8$ Hz, 4H, C_{4-H}, C_{4'-H}), 8.73 (d, $J=19.9$ Hz, 4H, C_{5-H}, C_{5'-H}), 8.42 (s, 4H, C_{6-H}, C_{6'-H}), 8.08 (m, 4H, C_{3-H}, C_{3'-H}), 7.57 (s, 4H, Ar-H), 7.31 (s, 3H, Ar-H), 4.08 (s, 3H, -OCH₃), 3.97 (s, 3H, -OCH₃) ppm.

^{13}C NMR (101 MHz, DMSO) δ 171.65, 158.53, 156.19, 155.58, 155.35, 155.28, 152.53, 151.40, 149.87, 147.64, 147.16, 138.51, 138.44, 138.01, 137.35, 130.46, 129.04, 128.19, 127.40, 126.78, 125.27, 125.08, 121.62, 121.46, 121.09, 118.45, 112.63, 111.63, 56.61, 56.25 ppm.

MS (MALDI) m/z calcd for $[\text{C}_{45}\text{H}_{34}\text{F}_{12}\text{N}_6\text{O}_4\text{P}_2\text{Ru}]$ (M)⁺: 1114.0969, found 1114.1991.

Biological Activity Investigations

Details of the hemolysis assay for assessing cytotoxicity, the *in vitro* anti-inflammatory albumin denaturation assay, the crystal violet assay for evaluating cell viability, and the antimicrobial activity tests are provided in the supporting information.

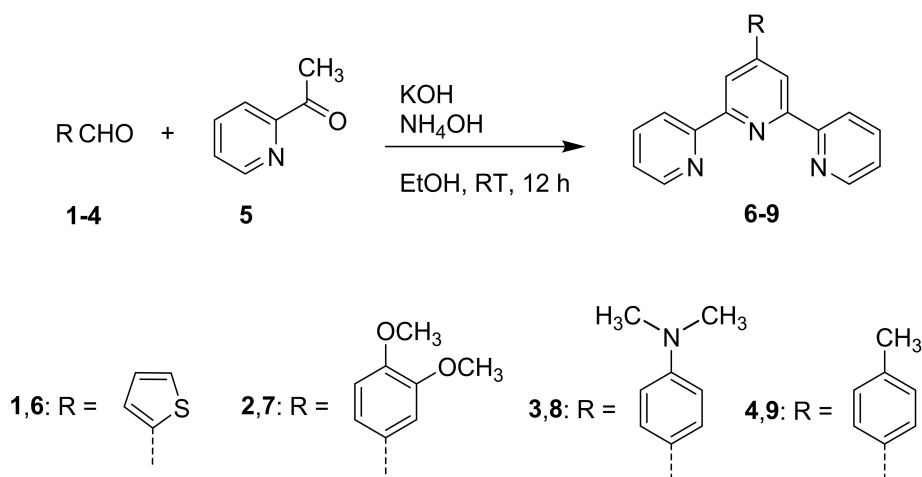
Results and Discussion

Synthesis

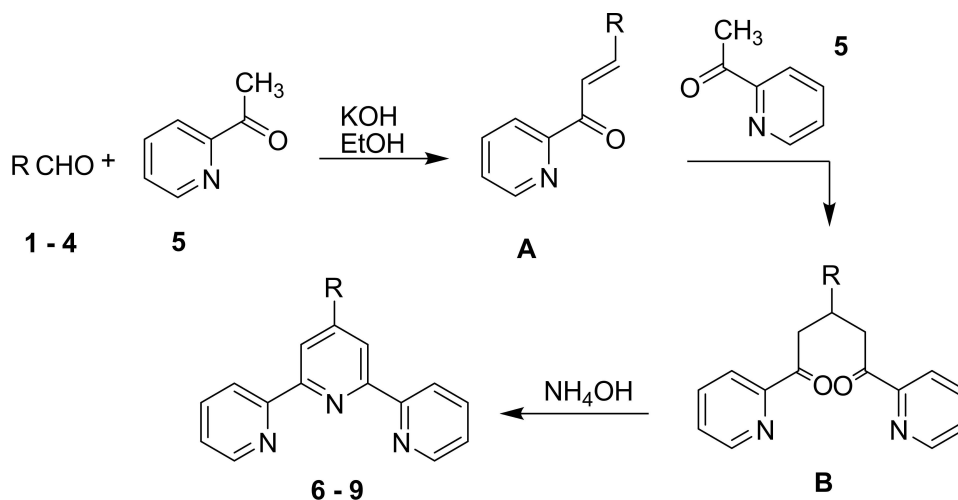
Although several synthetic routes have been proposed for the synthesis of 2,2':6',2''-terpyridine derivatives (tpy),^[30–33] the most common approach involves first synthesizing the intermediate 1,5-bis(pyridine-2-yl)pentane-1,5-dione, which is then cyclized to form the central pyridine ring using an ammonia source.^[34–36] Scheme 1 exhibits the standard approach employed for the synthesis of four terpyridine derivatives; 4'-(2-thienyl)-2,2':6',2''-terpyridine **6**, 4'-(3,4-dimethoxyphenyl)-2,2':6',2''-terpyridine **7**, 4'-(4-dimethylaminophenyl)-2,2':6',2''-terpyridine **8** and 4'-(4-

tolyl)-2,2':6',2''-terpyridine **9**. This method is regarded as a one-pot reaction, involving the condensation of 2-acetylpyridine **5** with thiophene-2-carbaldehyde **1**, 3,4-dimethoxybenzaldehyde **2**, 4-(dimethylamino)benzaldehyde **3** or 4-methylbenzaldehyde **4** under basic conditions to obtain terpyridine derivatives **6–9** before adding NH₄OH (Scheme 1). The postulated mechanism of formation of **6–9** is clearly illustrated in Scheme 2. The synthesis begins with the Kröhnke condensation of 2-acetylpyridine **5** with aldehyde derivatives **1–4** to produce the enone (chalcone) **A**. In the second step, a Michael addition of a second molecule of 2-acetylpyridine **5** to the condensation product **A** forms the 1,5-dione **B**. Finally, cyclization is achieved by treating **B** with ammonium hydroxide, which provides the ammonia needed for ring closure, resulting in the formation of the central pyridine unit and yielding the desired terpyridine ligands **6–9** (Scheme 2).

The heteroleptic complexes [Ru(4'-(2-thienyl)-2,2':6',2''-terpyridine)(4-(2,2':6',2''-terpyridine-4'-yl) benzoic acid)]²⁺ **14**, [Ru(4'-(3,4-dimethoxyphenyl)-2,2':6',2''-terpyridine)(4-(2,2':6',2''-terpyridine-4'-yl) benzoic acid)]²⁺ **15** and [Ru(4'-(4-



Scheme 1. Synthetic route for the synthesis of the terpyridyl ligands



Scheme 2. Detailed synthetic steps for the formation of terpyridine, highlighting the key intermediates

dimethylaminophenyl)-2,2':6',2''-terpyridine)(4-(2,2':6',2'' terpyridine-4'-yl) benzoic acid)]²⁺ **16** were successfully prepared in two steps, as illustrated in Scheme 3. Initially, terpyridine ligands **6–8** are reacted with RuCl₃·3H₂O in DMF as a solvent for 5 h to generate [Ru(4'-(2-thienyl)-2,2':6',2''-terpyridine)Cl₃] **11**, [Ru(4'-(3,4-dimethoxyphenyl)-2,2':6',2''-terpyridine)Cl₃] **12** and [Ru(4'-(4-dimethylaminophenyl)-2,2':6',2''-terpyridine)Cl₃] **13**. In the subsequent step, the complexes **11–13** are refluxing with 4-(2,2':6',2''-terpyridine-4'-yl) benzoic acid **10** (formed *via* oxidation of 4'-(4-Methylphenyl)-2,2':6',2''-terpyridine **9** using potassium dichromate and sulfuric acid) in DMF as a solvent for 8 h followed by addition of ammonium hexafluorophosphate to obtain the desired heteroleptic complexes **14–16** (Scheme 3).^[37,38] The Ru(II) complexes Ru(4'-(2-thienyl)-2,2':6',2''-terpyridine)(4-(2,2':6',2''-terpyridine-4'-yl) benzoic acid)](PF₆)₂, [Ru(4'-(3,4-dimethoxyphenyl)-2,2':6',2''-terpyridine)(4-(2,2':6',2''-terpyridine-4'-yl) benzoic acid)](PF₆)₂ and [Ru(4'-(4-dimethylaminophenyl)-2,2':6',2''-terpyridine)(4-(2,2':6',2''-terpyridine-4'-yl) benzoic acid)](PF₆)₂ are termed as RuTBCTS, RuTBCTMeO, and RuTBCTN, respectively.

Photophysical Characterizations

The absorption spectra of the newly synthesized complexes RuTBCTN, RuTBCTMeO, and RuTBCTS in acetonitrile are illustrated in Figure 2a. In the visible regime, these spectra cover a wide range (400–600 nm) with major absorption peaks at 502 nm, 494 nm, and 495 nm, respectively, which contribute to their deep red color. These peaks are primarily correlated to spin-allowed metal-to-ligand charge transfer (MLCT) transitions. The presence of this band in 4'-substituted-2,2';6',2''-tpy Ru(II) complexes is characteristic of an octahedral geometry, matching the ¹T_{1(g)} ← ¹A_{1(g)} transition.^[39,40] The molar extinction coefficients of complexes RuTBCTN, RuTBCTMeO, and RuTBCTS are 3.14×10⁴, 3.42×10⁴, and 4.02×10⁴ M⁻¹ cm⁻¹, respectively. These high absorbance values are attributable to the coordination of two terpyridine (tpy) ligands per Ru(II) center, which

enhances the overall π -conjugation. The extended π -conjugation is further facilitated by the 4-dimethylaminophenyl, thiophenyl, or 4-methoxyphenyl groups attached to the tpy ligands, as well as by the benzoic acid moiety on the other terpyridyl ligand. The absorption bands observed at wavelengths shorter than 400 nm are allocated to intraligand (π - π^*) charge transitions of the terpyridine ligands. The molar extinction coefficients of the complexes RuTBCTN, RuTBCTMeO, and RuTBCTS at 310 nm are 6.29×10⁴, 7.97×10⁴, and 8.32×10⁴ M⁻¹ cm⁻¹, respectively.

The stability of these synthesized complexes was also tested via UV-vis spectroscopy. The results revealed no significant spectral changes after one week at room temperature (25 °C), confirming their stability in their coordinating mode during biological activity investigations.

The emission spectra of the Ru(II) complexes in acetonitrile at 25 °C are demonstrated in Figure 2b. The proposed Ru(II) complexes display emission spectra that span a significant portion of the visible light regime upon excitation of the MLCT bands. The MLCT bands for the complexes are observed at approximately 650 nm, 672 nm, and 670 nm for RuTBCTN, RuTBCTS, and RuTBCTMeO, respectively indicating the presence of a "Ru (terpy)" moiety, influenced by the chromophoric behavior of conjugated substituents at the 4'-position. Complexes RuTBCTMeO and RuTBCTS show two bands in their emission spectra. For RuTBCTMeO, there is a lower intensity band at approximately 650 nm and a slightly higher intensity band at around 735 nm. Similarly, RuTBCTS displays a lower intensity band at around 670 nm and another band with slightly higher intensity at approximately 730 nm. The luminescence properties of both complexes can be explained by the simultaneous phosphorescence from two non-degenerate ³MLCT excited states, each localized on different ligands within the heteroleptic complex.^[41,42]

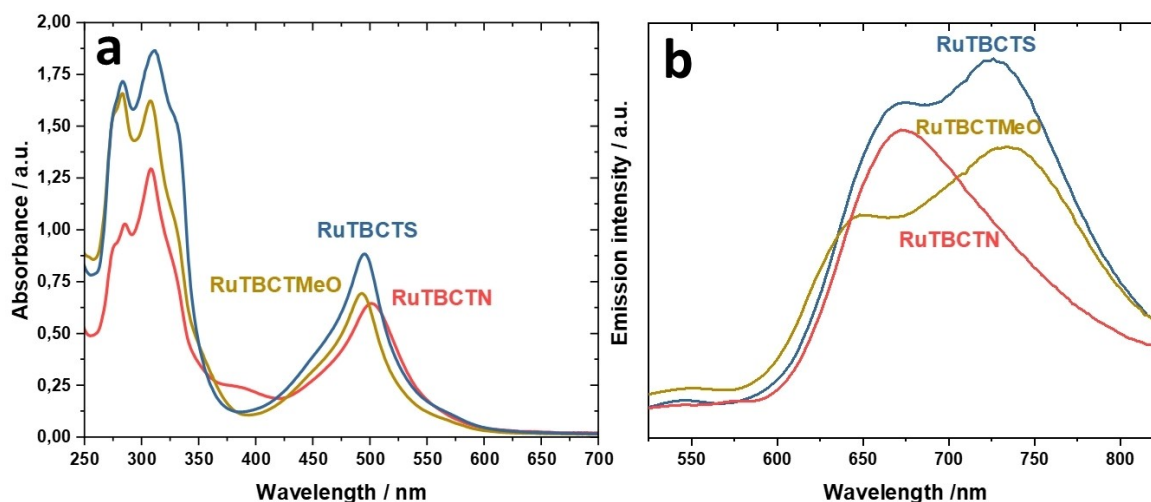
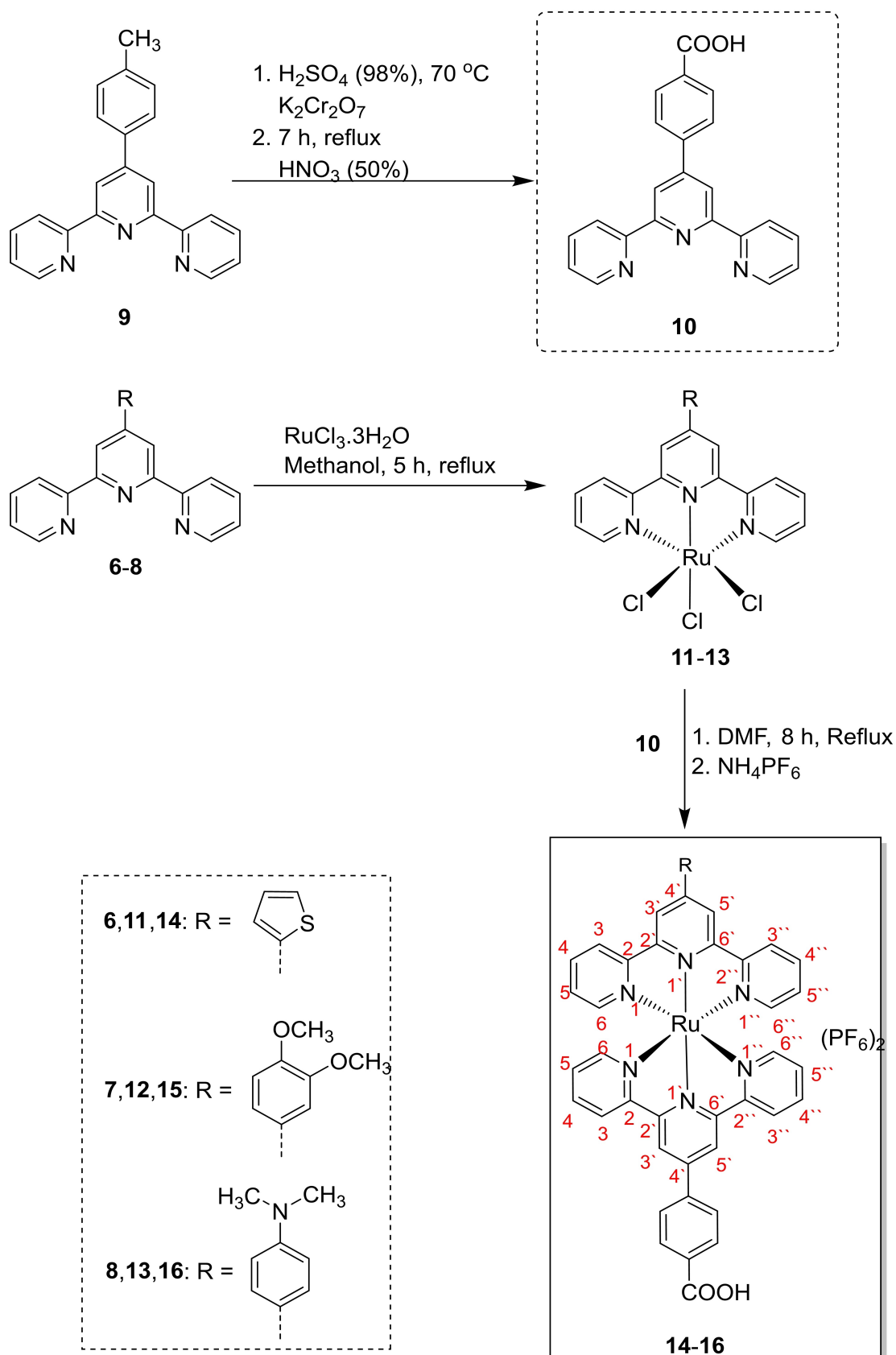


Figure 2. (a) Absorption and (b) emission spectra of RuTBCTN, RuTBCTMeO, and RuTBCTS recorded in acetonitrile.



Scheme 3. Synthetic steps of the heteroleptic ruthenium (II) complexes

Biological Investigations

Haemolysis Assay

Toxicity assessment is a crucial step in drug development, ensuring the safety and therapeutic potential of new compounds.^[43,44] We evaluated the toxicity of the proposed Ru(II) complexes through an in vitro hemolysis assay, benchmarked against diclofenac potassium and ibuprofen, as standard drugs (Figures 3a and b). Hemolysis, the rupture of erythrocytes and subsequent release of haemoglobin, serves as an indicator of cytotoxicity.^[45] Hemolytic activity is categorized by the mortality rate: non-toxic (0–9%), slightly toxic (10–49%), toxic (50–89%), and highly toxic (90–100%).^[46,47]

The Ru(II) complexes – RuTBCTN, RuTBCTS, and RuTBCTMeO – show slightly different toxicity profiles (Figure 3a). At 125 mg L⁻¹, only RuTBCTN is slightly toxic, while RuTBCTS and RuTBCTMeO remain non-toxic. At 250 and 500 mg L⁻¹, all three complexes are slightly toxic. In comparison, the standard drugs show notable levels of haemolysis, ranging from 54.5% to 58.0% for diclofenac potassium and 47.9% to 92.4% for ibuprofen at concentrations between 250 and 500 mg L⁻¹ (Figure 3b), consistent with their established toxicity profiles.^[55]

In contrast, the proposed compounds in this study exhibit much lower haemolytic activity, indicating greater safety margins compared to these drugs. These results emphasize the promising potential of these Ru(II) complexes for further pharmacological studies.

Inhibition of Albumin Denaturation and Anti-inflammatory Properties

To evaluate the in vitro anti-inflammatory activity of the Ru(II) complexes, their ability to inhibit heat-induced albumin denaturation was investigated and compared to standard drugs (ibuprofen and diclofenac potassium). The results are demonstrated in Figures 4a and b. At a concentration of 125 $\mu\text{g mL}^{-1}$, the Ru(II) complexes RuTBCTN, RuTBCTS, and RuTBCTMeO show inhibitory activities of 12.6%, 46.25%, and 36.9%, respectively. The inhibitory activity of the complexes increases significantly with increasing their amount, reaching a maximum of 90.3% for RuTBCTN and 100% for RuTBCTS and RuTBCTMeO at 500 $\mu\text{g mL}^{-1}$ (Figure 4a). The diclofenac potassium and ibuprofen inhibit heat-induced albumin denaturation by 88.37% and 51.5%, respectively, at 500 $\mu\text{g mL}^{-1}$, which is much lower than

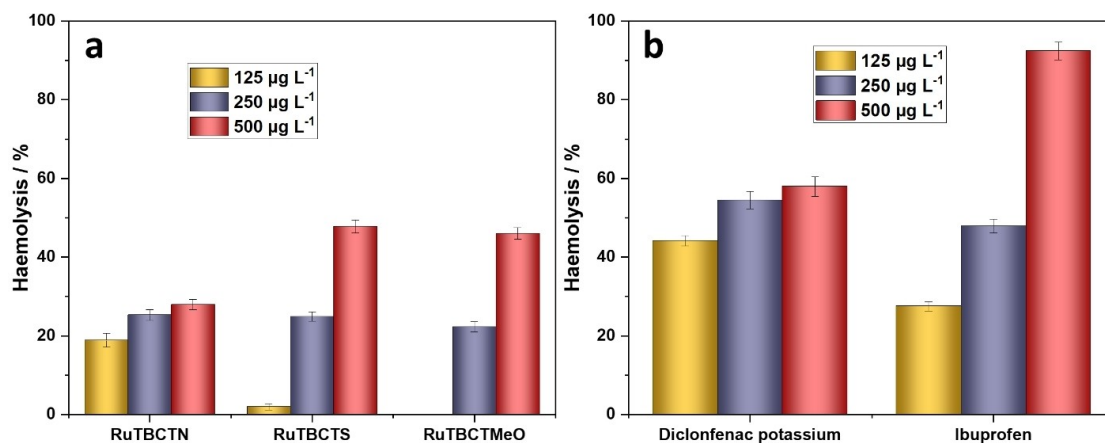


Figure 3. Effect of the (a) Ru(II) complexes and (b) standard drugs on the haemolysis of red blood cells (RBCs)

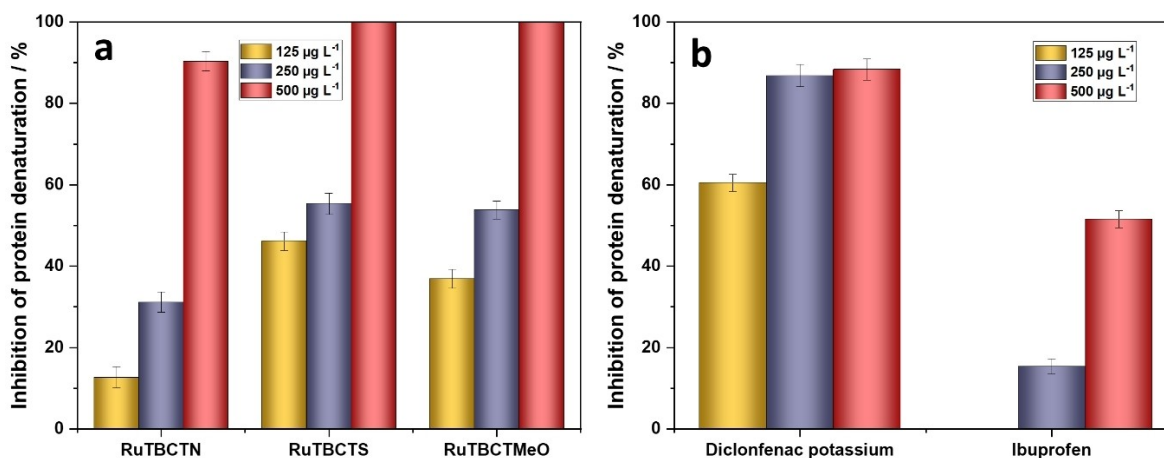


Figure 4. Activity of (a) the proposed Ru(II) complexes and (b) standard drugs in inhibiting heat-induced albumin denaturation

the proposed complexes (Figure 4b). Furthermore, the complexes with thiophene and 3,4-dimethoxyphenyl substituted groups are more effective in the inhibition of albumin denaturation than that of 4-dimethylaminophenyl.

Anticancer Activity

The in vitro cytotoxicity of the synthesized Ru(II) complexes was investigated using the crystal violet dye reduction assay. This assay was carried out using two human cancer cell lines (HepG2 and MCF-7) and one normal cell line derived from monkey kidney cells (Vero cells). DMSO was used as a solvent at concentrations below 2.5% (v/v), which are considered non-toxic to the cells. The concentration of each Ru(II) complex was 200 mg L⁻¹. The results are presented in Figure 5. Cytotoxic activity is categorized as follows: remarkable cytotoxic activity (> 75% of the cell population), moderate cytotoxic activity (40–75% of the cell population), low cytotoxic activity (0.1–40% of the cell population), and no cytotoxic activity (0% of the cell population).^[46] The Ru(II) complexes RuTBCTN, RuTBCTS, and RuTBCTMeO display varying levels of cytotoxic activity, influenced by the moieties on the 4'-substituted-2,2':6',2''-tpy ligands. The complex with the 3,4-dimethoxyphenyl moiety exhibits the highest cytotoxicity, followed by the complex with the thiophenyl moiety, and lastly, the one with the 4-dimethylaminophenyl moiety. These complexes also show higher selectivity against cancer cells compared to normal cells.

RuTBCTMeO demonstrates moderate cytotoxic activity against MCF-7 cells (41.0%) and lower cytotoxic activity towards HePG2 cells (32.5%) and Vero cells (21.1%). In comparison, the RuTBCTS and RuTBCTN complexes show low cytotoxic activity across all the investigated cell lines. Typically, Ru(II) terpyridine complexes exhibit cytotoxicity through several mechanisms: (i) robust binding to nucleic acids and proteins, (ii) ligand exchange processes, (iii) redox cycling between oxidation states II and III, and (iv) the ability of Ru(II) complexes to mimic iron in their interaction with biological molecules.^[1,5,27,49–52] Furthermore, terpyridine derivatives can induce DNA damage, disrupt calcium signaling, block receptor channels, and interact with proteins.^[53,54]

Antimicrobial Activity

Table 1 displays the antimicrobial activity of the proposed Ru(II) complexes in comparison with the standard drugs tetracycline and cycloheximide. The complexes were tested against *Aspergillus niger* NRRL A 326 (fungus), *Candida albicans* ATCC 10231 (yeast), *Pseudomonas aeruginosa* (Gram-negative bacterium), and *Staphylococcus aureus* ATCC 6538 (Gram-positive bacterium). Notably, the RuTBCTMeO complex exhibits the highest overall antimicrobial activity among the Ru(II) complexes, demonstrating significant broad-spectrum efficacy against all tested microorganisms. In contrast, the RuTBCTS complex shows high selectivity for *Aspergillus niger*, with no activity against *Candida albicans*, *Pseudomonas aeruginosa*, and Staph-

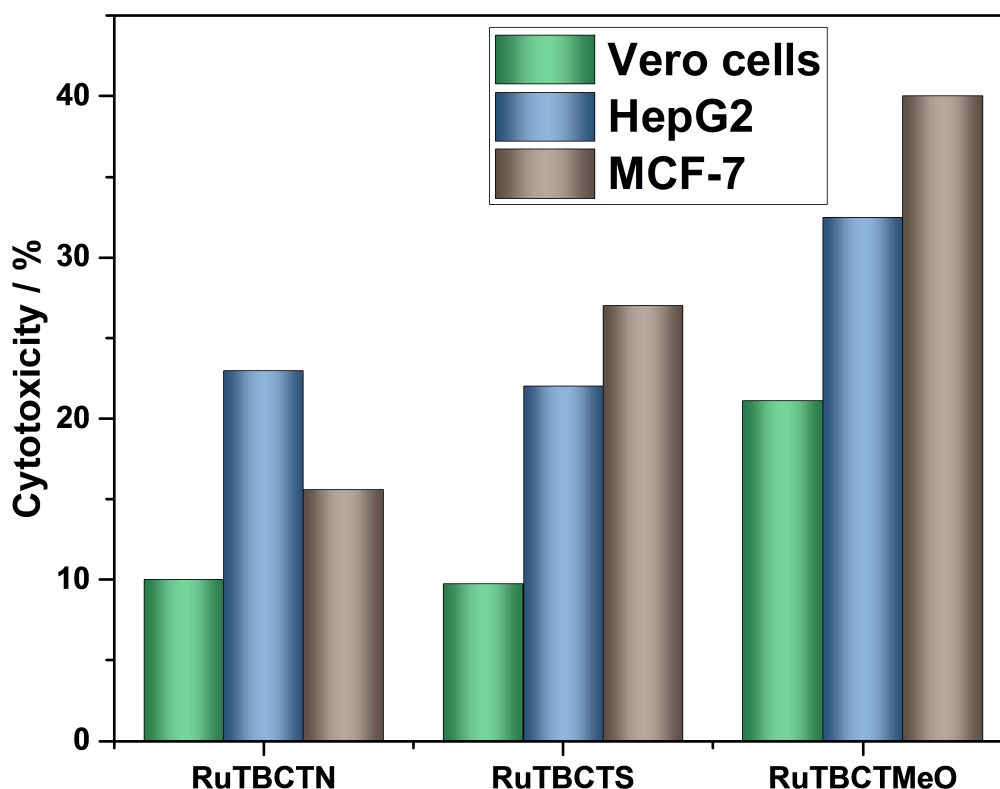


Figure 5. In vitro cytotoxic activity of the proposed Ru(II) complexes against Vero cells, HepG2, and MCF-7 cell lines

Table 1. Antimicrobial performance of the proposed Ru(II) complexes compared tetracycline and cycloheximide.

Compound	Clear zone/mm			
	<i>Aspergillus niger</i>	<i>Candida albicans</i>	<i>Pseudomonas aeruginosa</i>	<i>Staphylococcus aureus</i>
Tetracycline	0	28	34	36
Cycloheximide	39	0	0	0
RuTBCTN	0	21	23	18
RuTBCTS	25	0	0	0
RuTBCTMeO	32	23	24	21

Staphylococcus aureus. The RuTBCTN complex exhibits comparable antimicrobial activity to RuTBCTMeO against *Candida albicans*, *Pseudomonas aeruginosa*, and *Staphylococcus aureus* but lacks activity against *Aspergillus niger*. Overall, the RuTBCTMeO complex emerges as a promising candidate for antimicrobial applications, showing superior activity compared to the standard drugs tetracycline and cycloheximide, as well as some previously reported Ru(II) terpyridine complexes.^[55]

Conclusions

This study demonstrates the synthesis and characterization of three novel 4'-functionalized bis(terpyridine) Ru(II) complexes, (4'-(thiophen-2-yl)-2,2':6',2''-terpyridine) (4-([2,2':6',2''-terpyridin]-4'-yl)benzoic acid) Ru(II) di(hexafluoro- λ^6 -phosphane) (RuTBCTS), (4-([2,2':6',2''-terpyridin]-4'-yl)-N,N-dimethylaniline) (4-([2,2':6',2''-terpyridin]-4'-yl)benzoic acid) Ru(II) di(hexafluoro- λ^6 -phosphane) (RuTBCTN), and (4'-(3,4-dimethoxyphenyl)-2,2':6',2''-terpyridine) (4-([2,2':6',2''-terpyridin]-4'-yl)benzoic acid) Ru(II) di(hexafluoro- λ^6 -phosphane) (RuTBCTMeO). The absorption spectra of the complexes RuTBCTN, RuTBCTMeO, and RuTBCTS in acetonitrile show major peaks at 502 nm, 494 nm, and 495 nm, respectively, attributed to MLCT transitions, indicating octahedral geometry. The high molar extinction coefficients of the Ru(II) complexes result from the extensive π -conjugation of the tpy ligands. Emission spectra exhibit MLCT bands around 650 nm, 672 nm, and 670 nm for RuTBCTN, RuTBCTS, and RuTBCTMeO, respectively, with RuTBCTMeO and RuTBCTS showing a second emission band at 735 nm and 730 nm, respectively, likely due to phosphorescence from two non-degenerate ³MLCT excited states. Interestingly, these complexes exhibit diverse and robust biological activities. Biological assessments reveal low haemolytic potential, effective anti-inflammatory activity via the inhibition of thermal-induced albumin denaturation, selective cytotoxicity against cancer cells, and broad-spectrum antimicrobial effects. Particularly, the Ru(II) complex with 3,4-dimethoxyphenyl moiety on the terpyridine emerges as a promising candidate with the highest anti-inflammation activity and exceptional antimicrobial efficacy against multiple pathogens. These findings underscore the potential of 4'-functionalized bis(terpyridine) Ru(II) complexes as versatile therapeutic agents, addressing critical challenges in inflammation, cancer therapy, and infectious diseases. Further research is needed to optimize their pharmacological properties

and elucidate their mechanisms of action to facilitate clinical translation and application.

Acknowledgements

Open Access funding enabled and organized by Projekt DEAL.

Conflict of Interests

The authors declare no conflict of interest.

Data Availability Statement

Data will be made available on request.

Keywords: Ru(II) complexes · Terpyridine · Biological activity · Antimicrobial agents · Anti-inflammatory · Anti-cancer

- [1] I. Yousof, M. Bashir, F. Arjmand, S. Tabassum, *Coord. Chem. Rev.* **2021**, *445*, 214104.
- [2] E. A. Drweesh, V. Kuchárová, V. Volarevic, D. Miloradovic, A. Ilic, I. D. Radojević, I. R. Raković, R. Smolková, M. Vilková, D. Sabolová, M. M. Elnagar, I. Potočník, *J. Inorg. Biochem.* **2022**, *228*, 111697.
- [3] F. Li, J. G. Collins, F. R. Keene, *Chem. Soc. Rev.* **2015**, *44*, 2529–2542.
- [4] L. Conti, A. Mengoni, G. E. Giacomazzo, L. Mari, M. Perfetti, C. Fagorzi, L. Sorace, B. Valtancoli, C. Giorgi, *J. Inorg. Biochem.* **2021**, *220*, 111467.
- [5] M. Mital, Z. Ziora, *Coord. Chem. Rev.* **2018**, *375*, 434–458.
- [6] T. Ezhilarasu, S. Balasubramanian, *ChemistrySelect* **2018**, *3*, 12039–12049.
- [7] N. Alatrash, E. S. Narh, A. Yadav, M. Kim, T. Janaratne, J. Gabriel, F. M. MacDonnell, *ChemMedChem* **2017**, *12*, 1055–1069.
- [8] N. A. Yusoh, H. Ahmad, M. R. Gill, *ChemMedChem* **2020**, *15*, 2121–2135.
- [9] J. Husson, M. Knorr, *Beilstein J. Org. Chem.* **2012**, *8*, 379–389.
- [10] Y. Watanabe, R. Yoshioka, H. Sasabe, T. Kamata, H. Katagiri, D. Yokoyama, J. Kido, *J. Mater. Chem. C Mater.* **2016**, *4*, 8980–8988.
- [11] D. Mahendiran, R. S. Kumar, A. K. Rahiman, *Mater. Sci. Eng., C* **2017**, *76*, 601–615.
- [12] J.-L. Wang, X. Li, C. D. Shreiner, X. Lu, C. N. Moorefield, S. R. Tummalapalli, D. A. Medvetz, M. J. Panzner, F. R. Fronczek, C. Wesdemiotis, G. R. Newkome, *New J. Chem.* **2012**, *36*, 484.
- [13] C. Kreitner, M. Grabolle, U. Resch-Genger, K. Heinze, *Inorg. Chem.* **2014**, *53*, 12947–12961.
- [14] J. Saez, J. Quero, M. J. Rodriguez-Yoldi, M. C. Gimeno, E. Cerrada, *Inorg. Chem.* **2024**, DOI: 10.1021/acs.inorgchem.4c02988.
- [15] H. Yasir Khan, S. Parveen, I. Yousof, S. Tabassum, F. Arjmand, *Coord. Chem. Rev.* **2022**, *453*, 214316.
- [16] A. Tsoupras, S. Pafli, C. Stylianoudakis, K. Ladomenou, C. A. Demopoulos, A. Philippopoulos, *Compounds* **2024**, *4*, 376–400.

- [17] D. B. Farag, N. A. Farag, A. Esmat, S. A. Abuelezz, E. Abdel-Salam Ibrahim, D. A. Abou El Ella, *Medchemcomm* **2015**, *6*, 283–299.
- [18] D. Pires Gouvea, F. A. Vasconcellos, G. dos Anjos Berwaldt, A. C. P. S. Neto, G. Fischer, R. P. Sakata, W. P. Almeida, W. Cunico, *Eur. J. Med. Chem.* **2016**, *118*, 259–265.
- [19] R. K. Tonk, S. Bawa, G. Chawla, G. S. Deora, S. Kumar, V. Rathore, N. Mulakayala, A. Rajaram, A. M. Kalle, O. Afzal, *Eur. J. Med. Chem.* **2012**, *57*, 176–184.
- [20] S. Liu, J. Ren, P. ten Dijke, *Signal. Transduct. Target. Ther.* **2021**, *6*, 8.
- [21] F. R. Greten, S. I. Grivnennikov, *Immunity* **2019**, *51*, 27–41.
- [22] R. S. Y. Wong, *Int. J. Clin. Exp. Pathol.* **2021**, *15*;14, 831–844.
- [23] C.-H. Leung, S. Lin, H.-J. Zhong, D.-L. Ma, *Chem. Sci.* **2015**, *6*, 871–884.
- [24] F. Aman, M. Hanif, W. A. Siddiqui, A. Ashraf, L. K. Filak, J. Reynisson, T. Söhnel, S. M. F. Jamieson, C. G. Hartinger, *Organometallics* **2014**, *33*, 5546–5553.
- [25] E. K. Beloglazkina, A. G. Majouga, E. A. Manzheliy, A. A. Moiseeva, Y. V. Lin'kova, N. V. Zyk, *Polyhedron* **2015**, *85*, 800–808.
- [26] C. N. Banti, S. K. Hadjikakou, *Eur. J. Inorg. Chem.* **2016**, *2016*, 3048–3071.
- [27] M. M. Elnagar, S. Samir, Y. M. Shaker, A. A. Abdel-Shafi, W. Sharmoukh, M. S. Abdel-Aziz, K. S. Abou-El-Sherbini, *Appl. Organomet. Chem.* **2021**, *35*, e6024-undefined.
- [28] J. Wang, G. Hanan, *Synlett* **2005**, *2005*, 1251–1254.
- [29] B. A. Ali, W. Sharmoukh, M. M. Elnagar, Z. M. Hassan, N. K. Allam, *Appl. Organomet. Chem.* **2019**, *33*, e4677-undefined.
- [30] K. T. Potts, D. A. Usifer, A. Guadalupe, H. D. Abruna, *J. Am. Chem. Soc.* **1987**, *109*, 3961–3967.
- [31] Y.-W. Zhong, C.-J. Yao, H.-J. Nie, *Coord. Chem. Rev.* **2013**, *257*, 1357–1372.
- [32] D. L. Jameson, L. E. Guise, *Tetrahedron. Lett.* **1991**, *32*, 1999–2002.
- [33] H.-J. Park, Y. K. Chung, *Dalton. Trans.* **2012**, *41*, 5678.
- [34] J.-L. Wang, X. Li, C. D. Shreiner, X. Lu, C. N. Moorefield, S. R. Tummalapalli, D. A. Medvetz, M. J. Panzner, F. R. Fronczek, C. Wesdemiotis, G. R. Newkome, *New J. Chem.* **2012**, *36*, 484.
- [35] S. Wang, W. Chu, Y. Wang, S. Liu, J. Zhang, S. Li, H. Wei, G. Zhou, X. Qin, *Appl. Organomet. Chem.* **2013**, *27*, 373–379.
- [36] J. Wang, G. Hanan, *Synlett* **2005**, *2005*, 1251–1254.
- [37] I. M. Abdellah, A. I. Koraiem, A. El-Shafei, *Sol. Energy* **2019**, *177*, 642–651.
- [38] K. L. Vincent Joseph, A. Anthonysamy, R. Easwaramoorthi, D. V. Shinde, V. Ganapathy, S. Karthikeyan, J. Lee, T. Park, S.-W. Rhee, K. S. Kim, J. K. Kim, *Dyes Pigm.* **2016**, *126*, DOI: 10.1016/j.dyepig.2015.12.007.
- [39] D. W. Thompson, A. Ito, T. J. Meyer, *Pure Appl. Chem.* **2013**, *85*, 1257–1305.
- [40] Z. Ji, Y. Wu, *J. Phys. Chem. C* **2013**, *117*, 18315–18324.
- [41] E. C. Glazer, D. Magde, Y. Tor, *J. Am. Chem. Soc.* **2005**, *127*, 4190–4192.
- [42] E. C. Glazer, D. Magde, Y. Tor, *J. Am. Chem. Soc.* **2007**, *129*, 8544–8551.
- [43] A. M. B. Amorim, L. F. Piochi, A. T. Gaspar, A. J. Preto, N. Rosário-Ferreira, I. S. Moreira, *Chem. Res. Toxicol.* **2024**, *37*, 827–849.
- [44] F. Pognan, M. Beilmann, H. C. M. Boonen, A. Czich, G. Dear, P. Hewitt, T. Mow, T. Oinonen, A. Roth, T. Steger-Hartmann, J.-P. Valentin, F. Van Goethem, R. J. Weaver, P. Newham, *Nat. Rev. Drug Discov.* **2023**, *22*, 317–335.
- [45] F. Vallelian, P. W. Buehler, D. J. Schaer, *Blood* **2022**, *140*, 1837–1844.
- [46] T. Siriyong, J. C. Ontong, S. Leejae, S. Suwalak, P. J. Coote, S. P. Voravuthikunchai, *Toxicol. Rep.* **2020**, *7*, 919–924.
- [47] M. Pagano, C. Faggio, *Cell Biochem. Funct.* **2015**, *33*, 351–355.
- [48] J. López-García, M. Lehocý, P. Humpolíček, P. Sába, *J. Funct. Biomater.* **2014**, *5*, 43–57.
- [49] E. M. Hahn, N. Estrada-Ortiz, J. Han, V. F. C. Ferreira, T. G. Kapp, J. D. G. Correia, A. Casini, F. E. Kühn, *Eur. J. Inorg. Chem.* **2017**, *2017*, 1667–1672.
- [50] M. Nišavić, M. Stoiljković, I. Crnolatac, M. Milošević, A. Rilak, R. Masnikosa, *Arabian J. Chem.* **2018**, *11*, 291–304.
- [51] Y. Lu, Z. Hou, M. Li, N. Wang, J. Wang, F. Ni, Y. Zhao, B. Zhang, N. Xi, *Dalton Trans.* **2022**, *51*, 16224–16235.
- [52] C. G. Hartinger, M. Groessler, S. M. Meier, A. Casini, P. J. Dyson, *Chem. Soc. Rev.* **2013**, *42*, 6186.
- [53] L.-X. Zhao, T. S. Kim, S.-H. Ahn, T.-H. Kim, E. Kim, W.-J. Cho, H. Choi, C.-S. Lee, J.-A. Kim, T. C. Jeong, C. Chang, E.-S. Lee, *Bioorg. Med. Chem. Lett.* **2001**, *11*, 2659–2662.
- [54] K. S. Hsu, W. M. Fu, S. Y. Lin-Shiau, *Br. J. Pharmacol.* **1993**, *110*, 163–168.
- [55] T. Ezhilarasu, A. Sathiyaseelan, P. T. Kalaichelvan, S. Balasubramanian, *J. Mol. Struct.* **2017**, *1134*, 265–277.

Manuscript received: August 29, 2024

Revised manuscript received: October 15, 2024

Accepted manuscript online: October 17, 2024

Version of record online: November 21, 2024